Жидкие кристаллы и их практическое использование. 2022. Т. 22, № 3. С. 49–57
Liquid Crystals and their Application. 2022. Vol. 22, No. 3. P. 49–57
ISSN 1991–3966 (print), 2499–9644 (online), Journal homepage: http://nano.ivanovo.ac.ru/journal/ru/

Physics

Research Article
UDC 532.5, 532.6

SHEAR FLOWS INDUCED BY ELECTRO-OSMOTIC PUMPS IN OPTOFLUIDIC LIQUID CRYSTAL CELL FOR MODULATION OF VISIBLE LIGHT AND THZ IRRADIATION

S. V. Pasechnik[1]*, D. V. Shmeleva[1], A. Sh. Saidgaziev[1], S. S. Kharlamov[1], A. A. Vasilieva[1], S. Santer[2]

[1]*MIREA – Russian Technological University, Problem Laboratory of Molecular Acoustics, Moscow, Russia*
[2]*Institute of Physics and Astronomy, University of Potsdam, Potsdam, Germany*

A R T I C L E I N F O:

***Article history**:*
Received 30 May 2022
Approved 20 June 2022
Accepted 27 June 2022

***Key words**:*
nematic liquid crystal,
terahertz range,
electrokinetic phenomena,
osmotic flow,
director configuration,
optical irradiation intensity,
E7, polypropylene

A B S T R A CT

The work is devoted to the use of electrokinetic phenomena in liquid crystals to create a new class of microfluidics devices – optofluidics, designed to control electromagnetic radiation, including the THz frequency range. To achieve the goal, an optical method is used to study changes in the orientational structure in LC layers caused by a shear flow generated by electroosmotic pumps. Simulation of LC behaviour in an experimental cell containing electroosmotic pumps and flat layers of a nematic liquid crystal is fulfilled. The experimental dependences of the intensity of polarized radiation passing through flat LC layers on the control voltage applied to the electroosmotic pump and the results of calculations of the hydrodynamic and mechano-optical characteristics of the experimental LC cell are presented. The propagation of THz irradiation across the multilayer structure of the optofluidic cell is considered taking into account the minimum number of re-reflections of waves from different layers and the absorption of THz irradiation in a propylene and a liquid crystal.

DOI:
10.18083/LCAppl.2022.3.49

***For citation**:*
Pasechnik S. V., Shmeleva D. V., Saidgaziev A. Sh., Kharlamov S. S., Vasilieva A. A., Santer S. Shear flows induced by electro-osmotic pumps in optofluidic liquid crystal cell, for modulation of visible light and THz irradiation. *Liq. Cryst. and their Appl.,* 2022, **22** (3), 49–57.

*Corresponding author: s-p-a-s-m@mail.ru

Физика

Научная статья

СДВИГОВЫЕ ПОТОКИ, ВЫЗВАННЫЕ ЭЛЕКТРООСМОТИЧЕСКИМ НАСОСОМ В ОПТОЖИДКОСТНОЙ ЖИДКОКРИСТАЛЛИЧЕСКОЙ ЯЧЕЙКЕ, ДЛЯ МОДУЛЯЦИИ ВИДИМОГО СВЕТА И ТГц ИЗЛУЧЕНИЯ

С. В. Пасечник[1]*, Д. В. Шмелева[1], А. Ш. Саидгазиев[1], С. С. Харламов[1], А. А. Васильева[1], С. Сантер[2]

[1]МИРЭА – Российский технологический университет, Проблемная лаборатория молекулярной акустики, Москва, Россия
[2]Институт физики и астрономии Потсдамского университета, Потсдам, Германия

И Н Ф О Р М А Ц И Я

История статьи:
Поступила 30.05.2022
Одобрена 20.06.2022
Принята 27.06.2022

Ключевые слова:
нематический жидкий кристалл,
терагерцовый диапазон,
электрокинетические явления,
осмотический поток,
конфигурация директора,
интенсивность оптического излучения, E7,
полипропилен

А Н Н О Т А Ц И Я

Работа посвящена использованию электрокинетических явлений в жидких кристаллах для создания нового класса микрофлюидных устройств – оптофлюидики, предназначенных для управления электромагнитным излучением, в том числе терагерцового диапазона частот. Для достижения цели оптическим методом исследуются изменения ориентационной структуры в слоях ЖК, вызванные сдвиговым течением, генерируемым электроосмотическими насосами. Проведено моделирование поведения ЖК в экспериментальной ячейке, содержащей электроосмотические насосы и плоские слои нематического жидкого кристалла. Представлены экспериментальные зависимости интенсивности поляризованного излучения, проходящего через плоские слои ЖК, от управляющего напряжения, подаваемого на электроосмотический насос, и результаты расчетов гидродинамических и механооптических характеристик экспериментальной ЖК-ячейки. Рассмотрено распространение ТГц излучения по многослойной структуре оптофлюидной ячейки с учетом минимального числа переотражений волн от разных слоев и поглощения ТГц излучения в пропилене и жидком кристалле.

DOI:
10.18083/LCAppl.2022.3.49

Для цитирования:
Пасечник С. В., Шмелева Д. В., Саидгазиев А. Ш., Харламов С. С., Васильева А. А., Сантер С. Сдвиговые потоки, вызванные электроосмотическим насосом в оптожидкостной жидкокристаллической ячейке, для модуляции видимого света и ТГц излучения // *Жидк. крист. и их практич. использ.* 2022. Т. 22, № 3. С. 49–57.

*Автор для переписки: s-p-a-s-m@mail.ru

Introduction

In spite of the outstanding success achieved via usage of liquid crystals in the display industry, the unique properties of such materials attract also a growing interest for additional areas of practical applications [1]. In particular, it is well known that not only magnetic and electric fields, but also shear flows can induce the changes in the initial orientation of the local optical axis (director) initially stabilized by surfaces. Such changes result in corresponding variations of optic properties of LC layers-mechano-optical effects, which are interesting for elaboration of LC sensors of mechanical stress, pressure gradient and acceleration [2]. The orientation action of shear flows can be also considered as an alternative (respectively to usage of electric fields) way to control the light, propagating through LC layers. Such possibility was confirmed experimentally at optical investigations of steady and oscillating shear flows of LC. Recently the modulation of light via oscillating flow of LC, was realized on the base of a microfluidic chip, which was announced as an example of a new class of optofluidic devices. The usage of such devices for modulation of THz irradiation is of a special interest, as high energy losses in the ITO electrodes prevent the application of traditional electrical control in this frequency range and alternative control via usage of magnetic field [3] is too slow.

Recently, the general hydrodynamic schema of integrated LC optofluidic cell, which included electroosmotic pumps and plane channels was proposed and analyzed [4]. The results of the preliminary experimental investigation and computer modelling of the cell with electroosmotic pumps based on the usage of polymer porous films confirmed the general theoretical approach.

In this paper, we present the results of experimental investigation of a similar LC cell that can be used both in visible and in THz frequency ranges due to the usage of polymer substrates, which show, contrary to the previously used glass substrates, low absorption of the THz irradiation. So, such cell can be considered as a real prototype of the modulator for this frequency range. We also performed the computer simulation for THz irradiation when the wavelength was comparable with the thickness of different layers, passed by the wave. The obtained frequency dependencies of the total reflection coefficient can be used for optimization of LC optofluidic modulators operating in THz range. modulators of the THz frequency range [5, 6]. This made it possible to propose a new type of optofluidic liquid crystal modulator, which includes an electroosmotic pump that produces electroosmotic flows, as well as a number of flat channels with a given initial orientation.

Materials, design and principle of operation of an optofluidic cell

In this work, a nematic liquid-crystal mixture E7 (Fig. 1) [7] was chosen as an object of an investigation. This mixture has a wide temperature range (15–50 °C) of the nematic phase in the comparison with a nematic range (19–34 °C) of a liquid crystal 5CB, previously used in the similar investigation [5]. It is an important advantage for usage of such LC material in the prototypes of technical devices. In addition, there is abundant literature information on the physical properties of this mixture (including the refractive index and absorption coefficient in the THz range), which makes it possible to carry out mathematical modelling of the phenomena under consideration.

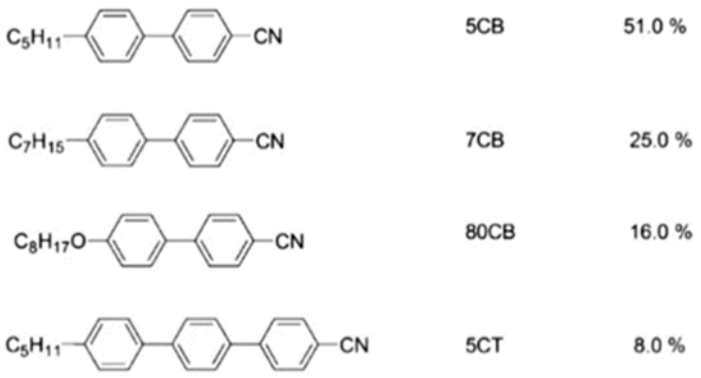

Fig. 1. Composition of LC E7 and molecular structure of the components

Note that E7 is characterized by a relatively large refractive index anisotropy in the THz frequency range ($\Delta n = (n_e - n_o) = 0.13$) [8], which is important for an effective phase modulation of electromagnetic radiation. Material parameters of E7, used in the modelling are presented in Table 1.

Table 1. **Material parameters of LC E7**

Material parameters	Value
Mesovich coefficient, η_1 [Pa·s]	0.264
Rotational viscosity, γ_1 [Pa·s]	0.224
Frank modulus, K_{33} [N]	$17.5 \cdot 10^{-12}$
Principal values of the permittivity tensor, $\varepsilon_\perp$/ $\varepsilon_\parallel$	2.61 / 3.03
Refractive index of the extraordinary wave (for 1 THz), n_e	1.73
Refractive index of an ordinary wave (for 1 THz), n_o	1.6
Absorption coefficient (for 1 THz), α [sm^{-1}]	18

Previously, in similar experiments [5], glass substrates were used, which have low absorption in the visible wavelength range. However, this material is not suitable for use in the THz frequency range due to the high absorption coefficient. In this regard, in the design of the LC cell described below, polymer substrates (*polypropylene*) were used. This material is characterized by a relatively low absorption in the THz frequency range ($\alpha = 0.58$ cm^{-1} at 1 THz) [9].

The optofluidic cell (Fig. 2) consists of two electroosmotic pumps, located in the terminal parts of the cell, and two plane capillaries, formed in the central part of the cell. Each pump includes a sample of a porous *polyethylene teraftalate* (*PET*) film with a thickness of 23 μm and an area of $S = 0.6$ cm^2 with a large number of identical submicron open-end pores with a diameter of $d = 0.5$ μm, oriented along the normal (z axis) to the film plane. The film is located between two electrodes made of thin copper foil with a thickness of 40 μm. Application of DC voltage U to the electrodes results in arising of an electric field E_i, directed along the pores, which induces electroosmotic flows inside the pores.

In turn, this leads to arising of Poiseuille flows with parabolic velocity profiles $v(z)$ in two plane channels, each of a gap $h = 52$ μm, with an initial homeotropic orientation, formed by the polymer (*polypropylene*) substrates of a thickness of 400 μm and the central *polypropylene* substrate of a thickness of 120 μm. All substrates and PET films were pre-treated with 5 % solution of *chromolane* in *isopropanole* to obtain a homeotropic surface orientation.

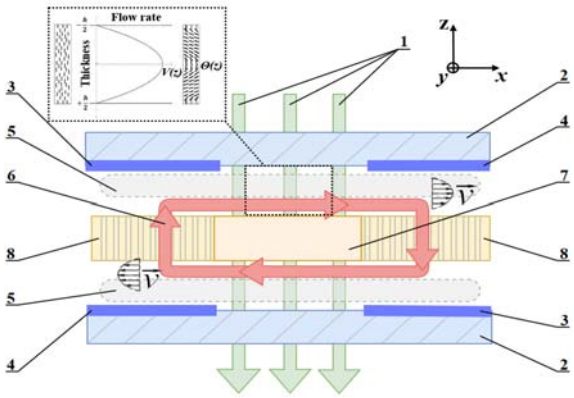

Fig. 2. Optofluidic cell scheme:
1 – modulated radiation, *2* – PP substrate, *3* – electrodes (+), *4* – electrodes (-), *5* – spacers, *6* – LC flow, *7* – PP partition, *8* – porous PET film

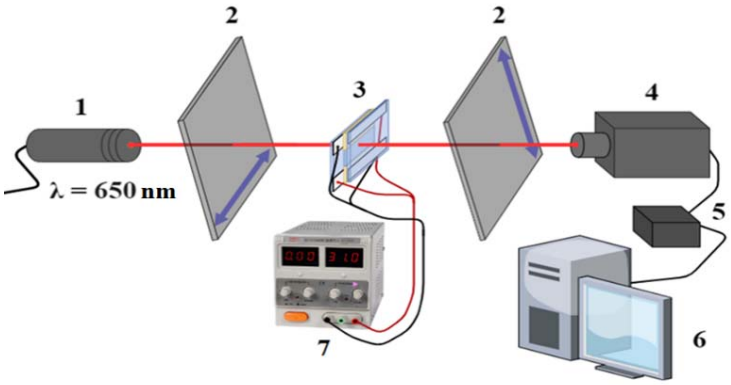

Fig. 3. Scheme of the experimental setup with a LC cell:
1 – laser radiation source, *2* – polarizers, *3* – LC cell, *4* – photodetector, *5* – ADC unit (L-card), *6* – personal computer, *7* – power supply

The experimental setup, shown in Fig. 3, was mounted on the optical bench. The cell was placed between two crossed polarizers oriented at an azimuthal angle of 45° relative to the direction of the LC flow through the plane channels.

The Poiseuille flows into plane channels, arising due to the action of electroosmotic pumps, led to a deviation of the orientation from initial homeotropic structure and the corresponding changes in the intensity of light with a wavelength of 650 nm. These changes were registered by a photodiode and, after being converted into a digital signal, entered the computer for storing and processing information using the L-CARD program.

The key effect responsible for the changes in light intensity is the flow induced birefringence which results in the phase delay δ between the ordinary and extraordinary beams due to an anisotropy of the refractive index. The arising of phase delay induces the changes ΔI in the intensity I of light, passed through homeotropic layers of LC cell, placed between crossed polarizers, described by the well-known expression (1):

$$\Delta I = I_0 \sin^2\left(\frac{\delta}{2}\right), \quad (1)$$

where I_0 – the input intensity of polarized light, $\Delta I = I$ – for perfect initial homeotropic orientation, $\delta = 2\delta_1$ – the phase delay in light wave arising at passing each LC layer, which is expressed as (2):

$$\delta = \frac{2\pi}{\lambda}\int_0^d (n_e(z) - n_o)dz = \frac{2\pi d\langle \Delta n(z)\rangle}{\lambda}, \quad (2)$$

where n_o – refractive index of an ordinary ray which will remain unchanged, $n_e(z)$ – the refractive index of the extraordinary ray that depends on the angle $\theta(z)$ between the director and z axis (3):

$$n_e(z) = \frac{n_o n_e}{\sqrt{n_o^2 sin^2\theta(z) + n_e^2 cos^2\theta(z)}}. \quad (3)$$

Experimental results

Fig. 4 shows the time dependences of light intensity on time, obtained when the control voltage U is turned on and off.

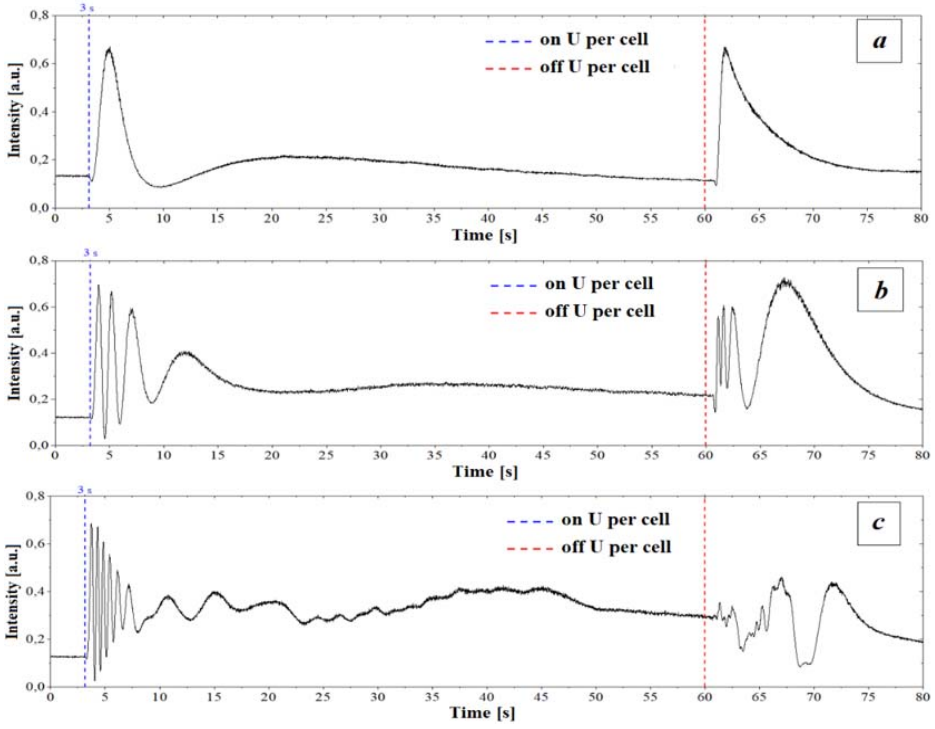

Fig. 4. Dependences of intensity on time I(t) at various voltages:
(*a*) U = 6 V, (*b*) U = 10 V, (*c*) U = 14 V

During the experiment, a constant voltage up to 20 V was applied to the cell. The main condition for choosing the experimental dependences corresponding to the director linear motion in the flow plane was the absence of distortion of the intensity oscillations. Such distortions took place both after turning on and off the voltage on the director return to original orientation. In our experiments, the linear regime was observed in the voltage range 6…10 V. At higher voltages, distortions of the time dependences took place, which can be explained by the escape of a director from the flow plane and the appearance of long-lived hydrodynamic instabilities [1].

The processing of the primary dependences *I(t)* made it possible to determine the time dependences (Fig. 5) of the phase difference δ*(t)* between the ordinary and extraordinary beams according to formula (4):

$$I(t) = I_0 * sin^2 2\varphi * sin^2 \frac{\delta(t)}{2}, \quad (4)$$

where $sin^2 2\varphi = 1$.

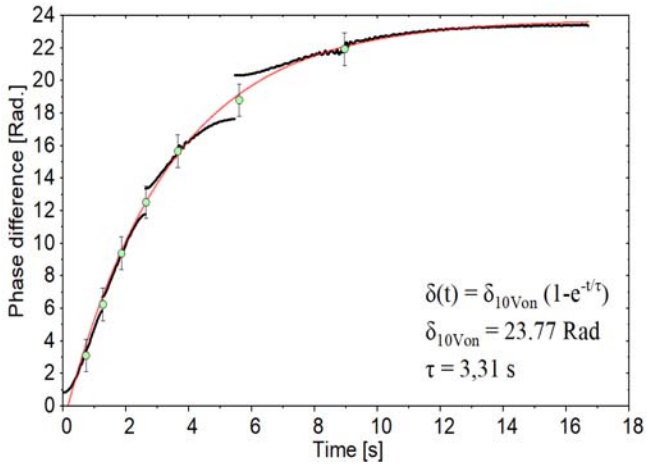

Fig. 5. Dependence of the phase delay δ*(t)* on time after application of the control voltage *U* = 10 V; Discontinuous black curves and green dots/marks are obtained by processing of *I(t)* dependences by expression (4) taking into account the time positions of maximum and minimum values of *I(t)*. Red solid curve corresponds to approximation of experimental data by formula (5)

The experimental dependence is well described by the exponential law (5), which corresponds to the solid line in Fig. 5:

$$\delta(t) = \delta_{max} \left(1 - e^{-\frac{t}{\tau}}\right). \quad (5)$$

The obtained characteristic time τ = 3.31 s is close to the theoretical value (τ_n = 3.46 s) of the director relaxation time to the initial state without taking into account the back flow (6):

$$\tau_n = \frac{\gamma_1 * h^2}{\pi^2 * K_{33}}. \quad (6)$$

Simulation results of optofluidic cell operation

The simulation was carried out on the basis of the previously proposed hydrodynamic model [5], which includes internal Z_i and external Z_e hydrodynamic resistances connected in series.

The volume flow Q_i generated in each pore of the electroosmotic pump is proportional to the axial component E_z of the electric field strength and can be expressed as:

$$Q_i = -(\varepsilon_0 * \varepsilon * \xi)\left(\frac{\pi * R^2}{\eta}\right) * E_z, \quad (7)$$

where $R/l_D >> 1$, η is the shear viscosity of the fluid in the pore, ξ – the zeta potential, l_d – the Debye length which characterizes the thickness of the near-surface layer with an inhomogeneous distribution of ions.

The total volumetric flow rate Q of the LC flow is expressed as:

$$Q = \frac{Q_i N_0 S}{(1 + r)}, \quad (8)$$

where $r = Z_e/Z_i$, N_0 – the surface density of pores in films, S – the area of porous film used in a pump.

The flow induced angle Θ(z) of director deviation from the initial homeotropic orientation (see Fig. 2) in each plane channel can be written as:

$$\Theta(\tilde{z}) = \frac{\alpha_2 * G}{6K_{33} * \eta_1} * z * \left(z^2 - \frac{h^2}{4}\right), \quad (9)$$

where in the case of small value of the flow induced angle Θ(z), $\alpha_2 \approx \gamma_1$ ($\eta_2 \approx \eta_1 - \gamma_1$), η_2 – minimal Mesovich coefficient.

The pressure gradient *G,* which provides the Poiseuille flows in the plane channel, is given by:

$$G = \frac{Q * 12\eta_1}{h^3 * A}, \quad (10)$$

where *h* and *A* – the channel's gap and width.

The phase difference δ at passing the light through two LC layers is expressed as:

$$\delta = \frac{2 * \pi * 2h}{\lambda} * \frac{n_0(n_e^2 - n_0^2)}{2n_e^2} * \langle \Theta^2 \rangle, \qquad (11)$$

where n_o and n_e are the refractive indexes of the ordinary and extraordinary waves; $<\Theta^2>$ is the averaged square of the angle Θ of the director deviation from the initial homeotropic orientation; λ is the wavelength of the light passing through the cell.

Fig. 6 shows the dependencies of calculated parameters on the electric field strength at variation of the LC's viscosity η inside a pore.

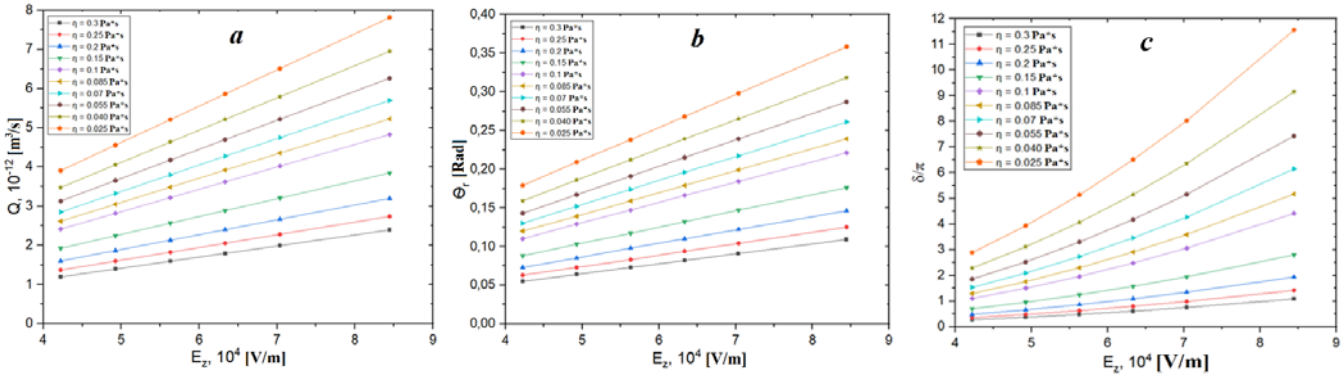

Fig. 6. Dependences of the parameters of the model on the electric field strength E_z in the pore: (*a*) volumetric flow rate; (*b*) the flow induced angle Θ of the LC director in the plane channel at $z = h/4$; (*c*) the phase difference δ between ordinary and extraordinary rays

Calculated dependences of the maximal value of the phase difference δ_{max} on electric field strength are shown in Fig. 7. These dependences are in agreement with the experimental data at values of the shear viscosity about 0.1 *Pa*s* inside pores. These values are in the range between minimal (0.04 *Pa*s*) and maximal (0.264 *Pa*s*) Mesovich coefficients [10]. So, the obtained value 0.1 *Pa*s* corresponds to non-homogeneous orientation of LC like radial escaped configuration [11].

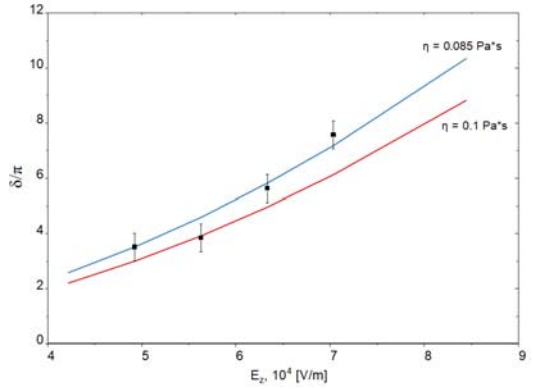

Fig. 7. Comparison of experimental data (squares) and theoretical dependences (solid lines) of the stationary phase difference δ on the field strength E_z at different values of the shear viscosity η of LC inside a pore

This makes it possible to propose the usage of such type of optofluidic device for modulation of electromagnetic waves in different frequency ranges including THz irradiation.

In the latter case, the wavelength can be comparable with the thickness of polymer substrates and LC layers. It makes calculation of the THz wave propagation through the multilayer structure (layers E7 and PP) more complicated than for the case of visible light. In particular, it is important to estimate effects of multiple reflections and absorption taking place in the optofluidic cell. The solution to this problem was based on the approach [12] proposed for calculation of light reflection from multilayer structures consisting of dielectric layers of different thickness and reflection indexes.

The main physical idea is to take into account the minimum number of re-reflections within the multilayer system. This is explained by the fact that the Fresnel reflection coefficients $r_{j,j+1}$ at the boundaries of two different media must satisfy the condition $|r_{j,j+1}| < 1$. This is precisely due to partial waves arising at re-reflections inside a layered system, which contribute to the sum of reflection coefficients.

The first approximation proposed in [12] results in the next expression for the total reflection coefficient $R_m^{(1)}$ of multilayer structure:

$$R_m^{(1)} = \sum_{j=0}^{m} \left(r_{j,j+1} \prod_{t=0}^{j} exp(2ik_{tz}d_t) \right), \qquad (12)$$

where m – the number of layers, $r_{j,j+1} = \frac{n_j - n_{j+1}}{n_j + n_{j+1}}$ – reflection coefficient on the boundary between two adjacent media, $k_{tz} = \frac{2\pi * f * n_x}{c_0}$ – incident wave vector.

The wave vector k for each layer is the sum of the real part describing the wave propagation velocity and the imaginary part equal to the absorption coefficient α of the material in this layer. The results of calculation of the energy reflection coefficients for ordinary and extraordinary rays propagating through the five-layer structure of the optofluidic cell without account of absorption are shown in Fig. 8.

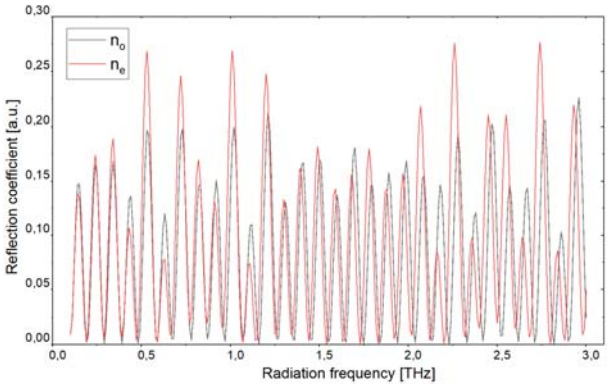

Fig. 8. Dependences of the reflection coefficient on the frequency of THz radiation for two values of refractions index corresponding to ordinary (n_o) and extraordinary (n_e) waves

It is worthwhile to notice that the maximal value of the flow induced variations of the polar angle Θ in a linear regime (typically of order π/4) is smaller than the value π/2, used at the presented above calculations. It results in decreasing the modulation of reflective light intensity.

The results of a simulation, which demonstrate the influence of absorption on the total reflection coefficients R_o and R_e of ordinary and extraordinary rays are presented in Table 2.

For the calculation, we used the data of previously reviewed works, where the absorption coefficients were studied in detail at different THz ranges of *polypropylene* and LC E7 [7, 8].

Table 2. **Comparison of the energy reflection coefficients in the presence and absence of absorption**

Value THz	R_o	R_o with abs.	R_e	R_e with abs.
1	0.14	0.098	0.246	0.194
1.25	0.039	0.036	0.01	0.021
1.5	0.17	0.102	0.167	0.115
1.75	0.001	0.012	0.064	0.047
2	0.148	0.083	0.051	0.049

The presented results show decreasing in the energy reflection coefficient in both cases, which is due to the energy losses in polypropylene and LC E7. In spite of the relatively small thickness of LC layers, they introduce an essential contribution in the reflection coefficient because of the higher values of absorption coefficient α in the comparison with the corresponding values of α for polypropylene.

Conclusion

The first experimental data on light modulation with the help of optofluidic LC cell including electroosmotic pumps and plane channels with polymer substrates are presented. These data are analyzed taking into account the electroosmotic flow, which results in changes of the initial homeotropic orientation of LC in plane channels.

Such changes induce the phase delay between ordinary and extraordinary rays, propagating through the cell, and lead to the variation of light intensity. The analysis of experimental data shows satisfactory agreement with the theoretical predictions.

The presented results indicate the possibility of elaboration of various terahertz devices (modulators, filters, etc.) based on optofluidic cells of the proposed type due to the difference of reflection coefficients for ordinary and extraordinary rays.

Acknowledgments. *This work was supported by the Ministry of Education and Science of Russian Federation (Grant № FSFZ-2020-0019) and Russian Foundation for Basic Research (RFBR and DFG project № 20-52-12040 and RFBR project № 19-32-90055).*

References

1. Pasechnik S.V., Chigrinov V.G., Shmeliova D.V. Liquid Crystals: viscous and elastic properties in theory and applications. W.: Wiley-VCH, 2009. 436 p. ISBN: 978-3-527-40720-0.

2. Vasdekis A.E., Cuennet J.G., De Sio L., Psaltis D. Optofluidic modulator based on peristaltic nematogenmicroflows. *Nature Photonics*, 2011, **5,** 234–238. **DOI**: 10.1038/NPHOT.2011.18.
3. Pasechnik S.V., Shmeliova D.V. Terafluidic devices-perspectives and problems. *IEEE 40-th International Conference on Infrared, Millimeter and Terahertz Waves.* 2015. 2 p. **DOI**: 10.1109/IRMMW-THz.2015.7327669.
4. Pasechnik S.V., Shmeliova D.V., Kharlamov S.S., Semina O.A., Saidgaziev A.Sh., Chigrinov V.G. Electrorheology of liquid crystals. *Liq. Cryst. and their Appl.*, 2018, **18** (3), 89–93. **DOI**: 10.18083/LCAppl.2018.3.89.
5. Shmeliova D.V., Saidgaziev A.Sh., Kharlamov S.S., Visotsky A.S., Safonov M.A., Konovalova A.A., Pasechnik S.V. Liquid crystal optofluidic device based on electro-kinetic phenomena in porous polymer films. *Liq. Cryst. and their Appl.*, 2020, **20** (3), 72–79. **DOI**: 10.18083/LCAppl.2020.3.72.
6. Shmeliova D.V., Pasechnik S.V., Kharlamov S.S., Saidgaziev A.Sh., Podolsky V.A. Electrokinetic phenomena in homeotropic layers of nematic liquid crystal. *Liq. Cryst. and their Appl.*, 2021, **21** (3), 39–44. **DOI**: 10.18083/LCAppl.2021.3.39.
7. Selvaraj P., Subramani K., Srinivasan B., Hsu C.-J., Huang C.-Y. Electro-optical effects of organic N-benzyl-2-methyl-4-nitroaniline dispersion in nematic liquid crystals. *Scientific Reports*, 2020, **10** (1), id. 14273. **DOI**: 10.1038/s41598-020-71306-1.
8. Mavrona E., Chodorow U., Barnes M.E., Parka J., Palka N., Saitzek S., Blach J.-F., Apostolopoulos V., Kaczmarek M. Refractive indices and birefringence of hybrid liquid crystal – nanoparticles composite materials in the terahertz region. *AIP Advances*, 2015, **5**, id. 077143. **DOI**: 10.1063/1.49273922.
9. Fedulova E.V., Nazarov M.M., Angeluts A.A., Kitai M.S., Sokolov V.I., Shkurinov A.P. Studying of dielectric properties of polymers in the terahertz frequency range. *Progress in Biomedical Optics and Imaging – Proceedings of SPIE,* 2012, **8337**, id. 83370I. **DOI**: 10.1117/12.923855.
10. Wang H., Wu T.X., Gauza S., Wu J.R. and Wu S.-T. Method to estimate the Leslie coefficients of liquid crystals based on MBBA data. *Liquid crystals*, 2006, **33** (1), 91–98. **DOI**: 10.1080/02678290500446111.
11. Stewart I.W. The static and dynamic continuum theory of liquid crystals: a mathematical introduction. L.: Taylor & Francis, 2004. 330 p. ISBN: 0-7484-0896-7.
12. Morozov G.V., Maev R.Gr., Drake D. Multiple reflection method for electromagnetic waves in layered dielectric structures. *Quantum Electronics,* 2001, **31** (9), 767–773. **DOI**: 10.1070/QE2001v031n09ABEH002042.

Contribution of the authors:

*[1]**Pasechnik S.V** – work management, analysis of theoretical material, correction of the textual material of the article;*
*[2]**Shmeleva D.V.** – consultation on planning, methodology and research implementation, writing the text of the article;*
*[3]**Saidgaziev A.Sh.** – conducting experiments, obtaining experimental data and calculating the obtained data;*
*[4]**Kharlamov S.S.** – data processing, graphing and drawing;*
*[5]**Vasilieva A.A.** – data processing, compiling, editing and translating the text of the work;*
*[6]**Santer S.A.** – consultation on planning, methodology and research implementation, writing the text of the article;*

The authors declare no conflicts of interests.

[1]*https://orcid.org/0000-0002-6050-2761*
[2]*https://orcid.org/0000-0003-3869-8806*
[3]*https://orcid.org/0000-0002-1815-2200*
[4]*https://orcid.org/0000-0002-6911-3228*
[5]*https://orcid.org/0000-0002-3151-6312*
[6]*https://orcid.org/0000-0002-5041-3650*

Received 30.05.2022, approved 20.06.2022, accepted 27.06. 2022